JVI Accepts, published online ahead of print on 3 September 2008
J. Virol. doi:10.1128/JVI.01454-08

Molecular and transmission characteristics of primary passaged ovine scrapie isolates in conventional and ovine PrP transgenic mice

Alana M. Thackray[1], Lee Hopkins[1], John Spiropoulos[2]

and Raymond Bujdoso[1]*

[1]Centre for Veterinary Science, Department of Veterinary Medicine

University of Cambridge, Madingley Road, Cambridge, CB3 OES, UK

[2]Neuropathology Unit, Department of Pathology, Veterinary Laboratories

Agency, Weybridge, New Haw, Addlestone, Surrey KT15 3NB, UK

*Corresponding author

(Tel: 44-1223-337655; Fax 44-1223-337610; email: rb202@cam.ac.uk)

Running title: Molecular and transmission characteristics of ovine prions

Word count: abstract – 250; total text – 7,090

Strains / polymorphism / transmissible spongiform encephalopathies / conformational / transgenic mice / immunoassay

ABSTRACT

A more complete assessment of ovine prion strain diversity will be achieved by complementing biological strain typing in conventional and ovine PrP transgenic mice with a biochemical analysis of the resultant PrPSc. This will provide a correlation between ovine prion strain phenotype and the molecular nature of different PrP conformers associated with particular prion strains. Here, we have compared the molecular and transmission characteristics of ovine ARQ/ARQ and VRQ/VRQ scrapie isolates following primary passage in *tg338* (VRQ) and *tg59* (ARQ) ovine PrP transgenic mice and the conventional mouse lines C57BL/6, RIII (both $Prnp^{a}$) and VM ($Prnp^{b}$). Our data show that these different genotypes of scrapie isolates display similar incubation periods of >350 days in conventional and *tg59* mice. Facilitated transmission of sheep scrapie isolates occurred in *tg338* mice with incubation times for VRQ/VRQ inocula reduced to 64 days, and to ≤210 days for ARQ/ARQ samples. Distinct genotype-specific lesion profiles were seen in the brains of conventional and *tg59* prion-diseased mice, which was accompanied by the accumulation of more conformationally stable PrPSc, following inoculation with ARQ/ARQ compared to VRQ/VRQ scrapie isolates. In contrast, the lesion profiles, quantities and stability of PrPSc induced by the same inocula in *tg338* mice were more similar than in the other mouse lines. Our data show that primary transmission of different genotypes of ovine prions is associated with the formation of different conformers of PrPSc with distinct molecular properties and provides the basis of a molecular approach to identify the true diversity of ovine prion strains.

INTRODUCTION

Prion diseases, such as scrapie of sheep, BSE of cattle and vCJD of humans are transmissible neurodegenerative disorders of the central nervous system. During the course of these diseases, host PrPC is converted into an abnormal isomer PrPSc. The protein-only hypothesis postulates that the transmissible agent comprises principally proteinaceous material (55). In this model, the infectious agent, or prion, is regarded as synonymous with PrPSc, which is also responsible for the conformational change in PrPC. However, different isolates of the prion agent obtained from individuals of the same species exhibit strain variation, reminiscent of strains of other conventional infectious agents, such as viruses. Different prion strains isolated upon serial passage through mice produce different disease phenotypes including incubation periods and lesion distributions (11, 13, 27, 32). These disease phenotypes, a feature of both the strain of the infectious prion agent and genetically encoded factors in the host, are typically stable on repeated passage through individuals of the same species. The strain-specific information of prions is therefore independent of the host from which they were originally derived. The phenomenon of prion strain variation has been a challenge to the protein-only hypothesis for prion diseases. Consequently, an alternative, less favoured, hypothesis is that the infectious prion agent carries a genome, and is a virus (18) or virino (31, 71) and suggests that the information that dictates prion strain diversity encoded by a molecule is independent of PrPSc.

Scrapie disease of sheep has been reported to exhibit a significant diversity of prion strains. The identification of ovine prion strains has typically involved serial passage of scrapie isolates in a panel of conventional mice including C57BL/6 and RIII (*Prnp*^{a}) and VM (*Prnp*^{b}) lines, and sometimes C57BL x VM F1 (10). This procedure has reportedly identified at least 14 scrapie prion strains and has enabled the BSE agent to be distinguished from scrapie (10-12). Significant drawbacks of this conventional approach to ovine scrapie prion strain typing are the large numbers of mice required, long incubation periods and the low efficiency of transmission in certain cases. Not all isolates of scrapie cause the appearance of clinical signs of prion disease in conventional mice (13)(and our own unpublished data). Approximately 20% of classical scrapie, and all atypical scrapie cases to date fail to transmit to the standard prion strain typing mouse lines. Even successful transmissions of classical scrapie samples may be characterized by low attack rates. The failure to see the onset of terminal disease may arise as a consequence of low dose of infectivity in the original prion inoculum or represent “adaptation” or “selection” of prions crossing the species barrier into a new host (30, 38-40). The absence of terminal disease in mice inoculated with different ovine prion strains is problematic for conventional strain typing as no incubation time can be recorded and neuropathology may not be evident. Efficient transmission of prions from different species has been achieved in mice that express a PrP transgene homologous to the host from which the prion isolates were obtained (9, 17, 24). Facilitated transmission of ovine scrapie strains to mice transgenic for either ovine ARQ (26) or VRQ PrP (69) has also been described. Mice transgenic for ovine VRQ PrP (*tg338* mice) show enhanced susceptibility, in terms of reduced incubation times to terminal disease, compared to conventional

mice after inoculation with prion inoculum from field cases of classical scrapie (43, 69). In addition, atypical strains of scrapie, which do not induce terminal prion disease in conventional mice, do induce terminal disease in *tg338* mice. Significantly, different scrapie isolates induced terminal disease in *tg338* mice with different incubation times and with distinct neuropathologies, which allows the potential for single-passage scrapie prion strain typing (6, 43). These features of ovine PrP transgenic mice highlight their potential utility in developing more rapid systems of ovine prion strain typing.

The qualitative features of different prion strains, which include clinical signs, lesion profile, brain distribution of PrPSc and western blot pattern of PrPSc do not presently explain or correlate with their quantitative traits such as incubation time and dose response. Safar et al (59) have successfully used a conformation-dependent immunoassay (CDI) to correlate conformational characteristics of PrPSc and its rate of accumulation with incubation time in eight prion strains propagated in Syrian hamsters. Each prion strain was found to produce a substantial fraction of protease-sensitive PrPSc, determined by CDI measurement of PrPSc before and after limited Proteinase K (PK) digestion. A significant correlation was found between the level of protease-sensitive PrPSc and the incubation time of the prion strain (59). This implies that different incubation times of various prion strains may arise as a consequence of distinct rates of PrPSc clearance rather than rate of PrPSc formation. This in turn suggests that different prion strains exhibit different conformational stability of PrPSc, which appears to be the case (53, 54). Determination of the conformational stability of an extensive panel of synthetic and naturally occurring prions passaged in mice

showed that the concentration of guanidine hydrochloride (GdnHCl) required to induce half-maximal denaturation correlated positively with their incubation time (44). These studies have begun to address the correlation of the biological properties of different prion strains with the biochemical properties of PrPSc.

In order to obtain a more complete understanding of the diversity of ovine prion strains it will be important to supplement the biological strain typing of scrapie isolates in mice with different PrP genotypes with a biochemical analysis of the resultant PrPSc. This will lead to a correlation between prion strain phenotype and the molecular nature of different PrP conformers associated with particular prion strains. Strain typing ovine scrapie isolates in wild type mice may lead to the generation of new prion strains as the original prions undergo “adaptation” or “selection” as a consequence of the infectious agent crossing the species barrier into a new host (1, 22). This may mean that lesion profiles at first passage in conventional mice do not reveal properties of the infectious prion agent as they exist in the original host. This should be circumvented if ovine scrapie isolates are passaged in ovine PrP transgenic mice. In order to address this we have for the first time compared the primary transmission characteristics of ovine ARQ/ARQ and VRQ/VRQ scrapie isolates in conventional and ovine PrP transgenic mice in order to investigate the biochemical and biophysical characteristics of PrPSc that originate from sheep prion isolates in hosts of different PrP genotypes. Our data show that although ARQ and VRQ homozygous scrapie isolates show similar incubation periods in conventional mice and ovine ARQ PrP transgenic mice, the quantity and nature

of deposited PrPSc shows significant variation. In contrast, these differences are not evident following transmission of the same inocula in ovine VRQ PrP transgenic mice. Our data show that primary transmission of different genotypes of ovine prions is associated with the formation of different conformers of PrPSc with distinct molecular properties and provide the basis of a molecular approach to identify the true diversity of ovine prion strains.

MATERIALS AND METHODS

Mice

Breeding colonies of the conventional mouse lines C57BL/6, RIII, VM and the ovine PrP transgenic mouse lines *tg59* (25) and *tg338* (69) were maintained at the VLA, Weybridge. All regulated procedures involving experimental animals were carried out under Project and Personal licence authority issued in accordance with The Animals (Scientific Procedures) Act 1986.

Inoculation of mice with ovine scrapie prion inoculum

Approximately 2g of cerebral cortex brain material from confirmed positive cases of ARQ/ARQ (n=2, SE1848/0007 and SE1848/0008) and VRQ/VRQ (n=2; SE1848/0005 and SE1848/0006) sheep with scrapie were homogenized and subsequently diluted in normal saline to produce a 10% wt/vol homogenate. Each scrapie isolate was from a different farm. Following confirmation of sterility by aerobic culture, each scrapie isolate was injected into 20 C57BL/6, RIII, VM, *tg59* and *tg338* mice by combined intra-cranial (20μl) and intra-peritoneal (100μl) routes. Mice were monitored for the development of clinical signs of mouse prion disease and were euthanized at the time of appearance of terminal signs of disease.

Histopathology and Immunohistochemistry

Brains from prion inoculated mice were isolated, a rostrolateral portion removed and stored frozen, and the remainder fixed in 10% formol saline. Haematoxylin and eosin stained sections at 5 coronal levels were examined for vacuolar pathology, to

168 determine lesion severity and distribution as described by Fraser and Dickinson (33).
169 Incubation time for terminal prion disease was calculated as the time from inoculation
170 to euthanazia at terminal prion disease. Attack rate for each mouse line was
171 calculated as the number of mice diagnosed positive divided by the number surviving
172 after, and including, the first positive diagnosis for each inoculum in a particular
173 mouse line. This avoids underestimation of the attack rate due to loss of mice as a
174 result of inter-current deaths early in the study. Incubation time for attack rate was
175 calculated as the time from inoculation to death or euthanazia (for whatever reason)
176 for prion-diseased-positive mice. Brain sections from prion-inoculated mice were
177 immunostained for PrP using rabbit anti-bovine PrP antiserum Rb486 as previously
178 described (37). At least 3 mouse brains were examined from each line of mice. For
179 each mouse, the patterns of disease-associated PrP deposition were recorded and
180 the presence of plaques noted.
181
182 **Anti-PrP monoclonal antibodies**
183 The anti-PrP monoclonal antibodies used here have been described in detail
184 elsewhere. Monoclonal antibody V24 recognizes an undefined epitope in the C-
185 terminal region of PrP (67). Monoclonal antibody 683 recognizes the core sequence
186 PVDQY (amino acid residues 168-172, ovine PrP numbering) (67). Monoclonal
187 antibody 6H4 reacts with the epitope DYEDRYYRE (amino acid residues 144 - 152,
188 human PrP numbering) (41) and was a generous gift from Prionics AG, Zürich,
189 Switzerland. Monoclonal antibody P4 reacts with the core sequence WGQGGSH
190 (amino acid residues 93 - 99, ovine PrP numbering) (68) and was purchased from R-

191 Biopharm, Darmstadt, Germany. Monoclonal antibodies were biotinylated as
192 described in detail previously (64).
193
194 **Conformation-dependent immunoassay (CDI)**
195 Murine sagittal-cut half-brain homogenates were prepared by two cycles of
196 homogenization in PBS (pH 7.4) in a Bio-Rad TeSeE Precess 24 homogenizer and
197 individual samples diluted to 10% in PBS supplemented with 1 mM 4-(2-
198 Aminoethyl)benzenesulfonyl fluoride (AEBSF) diluted in distilled water. Samples were
199 centrifuged at 100 x *g* for 1 min at 20 ˚C to remove gross debris and the supernatants
200 were retained. A final concentration of 2% sarkosyl in PBS (pH 7.4) was added to all
201 samples and incubated for 10 min at 37 ˚C with shaking prior to treatment ± sodium
202 phosphotungstic acid (NaPTA) at a final concentration of 0.4% diluted in PBS (pH
203 7.4) for 1 h at 37 ˚C with shaking. Samples were centrifuged at 21,000 x *g* for 30 min
204 at 10 ˚C, the supernatants were discarded and the pellets were re-suspended in 200
205 *µ*l 0.1% sarkosyl in PBS (pH 7.4) and 200 *µ*l 250 mM EDTA in water (pH 8.0).
206 Samples were thoroughly mixed and then centrifuged at 21,000 x *g* for 15 min at 10
207 ˚C. The supernatants were discarded and the pellets re-suspended in 0 M or 6 M
208 GdnHCl. All 6 M GdnHCl samples were then heated to 80 ˚C for 5 min, cooled to 20
209 ˚C and then diluted as required. Capture antibody diluted in coating buffer (0.01 M
210 PBS [pH 7.4] containing 0.1% sodium azide) was routinely coated at 0.5 *µ*g/well in
211 triplicate in Nunc Maxisorp 96-well flat-bottomed plates overnight at 4 ˚C. The
212 remainder of the CDI protocol was carried out as described in detail previously (64).
213 Plates were finally incubated for 5 min at 20 ˚C with shaking and the fluorescence,

214 measured as counts per second (cps), was determined in a Victor time-resolved
215 fluorimeter (PerkinElmer).
216
217 **Western blot detection of PrPSc**
218 100% ovine brain homogenates were diluted to 10% in Prionics Check Western
219 homogenization buffer prior to treatment with various concentrations of PK (Roche).
220 Murine sagittal-cut half-brain homogenates were prepared by two cycles of
221 homogenization in Prionics Check Western homogenization buffer in a Bio-Rad
222 TeSeE Precess 24 homogenizer. Brain homogenates were diluted to 10% in the
223 same buffer prior to treatment with PK at various concentrations for ovine scrapie
224 samples (see Figure 1) or at a final concentration of 32 μg/ml for C57Bl/6, RIII and
225 VM homogenates and 64 μg/ml for *tg59* and *tg338* homogenates. Digestion was
226 terminated with the addition of 1 mM AEBSF and samples were electrophorezed by
227 12% sodium dodecyl sulfate-polyacrylamide gel electrophoresis (SDS-PAGE) mini-
228 gel under reducing conditions and subsequently transferred onto a nitrocellulose
229 membrane by semi dry blotting. Membranes were blocked overnight at 4 ˚C with
230 TBS-T (10 mM Tris/HCl [pH 7.8], 100 mM NaCl, 0.05% Tween 20) containing 5%
231 (wt/vol) non-fat milk and subsequently washed three times with TBS-T. Membranes
232 were incubated with either purified anti-PrP monoclonal antibody 683 used at 5 μg/ml
233 (for detection of murine PrP) or P4 (R-Biopharm, Darmstadt, Germany) used at 1
234 μg/ml (for the detection of ovine PrP) for 2 h at 20 ˚C. The membranes were washed
235 five times with TBS-T followed by incubation with goat anti-mouse IgG-horseradish
236 peroxidase (Sigma) at 1:2000 for 2 h at 20 ˚C and a further five washes with TBS-T.
237 All of the antibody dilutions were prepared in 1% non-fat milk in TBS-T and the

duration of each wash step was 5 min. PrP bands were detected by enhanced chemiluminescence (Amersham Biosciences).

Conformational stability western blot

Murine sagittal-cut half-brain homogenates were prepared by two cycles of homogenization in PBS (pH 7.4) in a Bio-Rad TeSeE Precess 24 homogenizer. Brain homogenates were diluted to 10% in PBS (pH 7.4) prior to treatment with GdnHCl (0-2 M final concentration) for 30 min at 20 ˚C. The GdnHCl was diluted to a final concentration of 0.1 M with PBS (pH 7.4), prior to incubation with PK at a final concentration of 32 μg/ml for C57BL/6, RIII and VM homogenates or 64 μg/ml for *tg59* or *tg338* homogenates for 30 min at 37 ˚C. The reaction was terminated by the addition of 1 mM AEBSF, centrifuged at 16,160 x *g* and the pelleted material subsequently analyzed by SDS-PAGE and western blot. PrP bands were detected by enhanced chemiluminescence (Amersham Biosciences).

Statistical analysis

Statistical analyses of the data were performed using one-way ANOVA with Tukey HSD (honestly significant difference) for *post hoc* analysis or the two-tailed Student *t* test (unpaired samples) using the Prism 4 software package (GraphPad, San Diego, USA).

RESULTS

Transmission of ovine scrapie isolates to conventional and ovine PrP transgenic mice

Over several years numerous isolates of scrapie have been passaged as primary transmissions to a panel of conventional mice in order to determine strain diversity. Here we have compared primary transmission of sheep scrapie isolates in conventional and ovine PrP transgenic mice in order to determine whether the latter may contribute to the assessment of ovine prion strain diversity. The ovine ARQ/ARQ and VRQ/VRQ scrapie isolates used were from scrapie-positive sheep that showed typical vacuolar pathology in the medulla oblongata of the brain stem and that were positive for disease-associated PrP as judged by immunohistochemistry or western blot through routine statutory surveillance. Figure 1 shows a western blot analysis of representative ARQ and VRQ homozygous scrapie isolates, with or without PK digestion, probed with monoclonal antibody P4. The upper panel of Figure 1 shows that the PK-resistant core of PrPSc, PrP27-30, was present in both ARQ and VRQ homozygous ovine scrapie isolates at all concentrations of proteolytic enzyme tested. The lower panel of Figure 1 shows that both genotypes of scrapie isolate were characterized by a predominance of di-glycosylated PrP27-30. Although not formally quantified, it was apparent that the homozygous VRQ scrapie isolates exhibited more PrP27-30 compared to that seen in homozygous ARQ samples, which correlated with the greater level of total PrP in these samples.

The molecular and transmission characteristics of the various ARQ/ARQ and VRQ/VRQ scrapie isolates were determined following primary passage in C57BL/6, RIII (both *Prnp*^{a}), VM (*Prnp*^{b}), *tg59* (ovine ARQ) and *tg338* (ovine VRQ) mice. Following inoculation, animals from each of the various mouse lines developed prion disease, usually, but not always, accompanied by the appearance of typical clinical signs of this condition. Clinical signs of prion disease were least evident in prion-inoculated *tg59* mice. Table 1 shows the mean incubation time for the onset of terminal prion disease and the mean incubation time for attack rate. As shown in Table 1 most of the scrapie isolates produced similar incubation periods for the onset of terminal prion disease in the ovine ARQ PrP transgenic mouse line *tg59* and the conventional mouse lines, although there were exceptions. Furthermore, all of the inocula produced significantly accelerated incubation periods following inoculation into *tg338* mice, which are transgenic for ovine VRQ PrP. *Tg338* mice succumbed to terminal prion disease with very short incubation periods following inoculation with VRQ/VRQ scrapie isolates, approximately 64 days in both cases, which was significantly shorter than that seen for the same samples in C57BL/6 ($p<0.001$), RIII ($p<0.001$), or VM ($p<0.001$), mice. In a similar manner, *tg338* mice succumbed to terminal prion disease after relatively short incubation periods following inoculation with ARQ/ARQ scrapie isolates, 155 and 210 days, which was significantly shorter than that seen for the same samples in C57BL/6 ($p<0.001$), RIII ($p<0.001$) or VM ($p<0.001$) mice. Furthermore, the incubation times for the VRQ/VRQ scrapie isolates in *tg338* mice were significantly shorter than that seen for the ARQ/ARQ isolates in the same mouse line ($p\leq0.01$ in both cases). Despite similarities and differences in incubation periods for terminal prion disease, efficient attack rates were seen for all

305 inocula in all of the mouse lines. The attack rate range in RIII mice was 93 – 100%; in
306 VM mice 67 – 100%; in C57BL/6 and *tg59* mice was 100% in all four groups, and in
307 *tg338* mice the range was 92 – 100%.
308
309 All prion-inoculated mice were evaluated according to pre-determined protocols
310 established from the study of prion disease in wild type mouse lines (28). Clinical
311 signs of terminal prion disease were clearly evident in C57BL/6, RIII, VM and *tg338*
312 mice, which all showed a clear demarcation between early clinical disease and signs
313 of terminal prion disease. With respect to prion-inoculated *tg59* mice, these animals
314 showed signs of prion disease that persisted over a long period of time and did not
315 show the same signs of terminal prion disease, as did all of the other mouse lines.
316 *Tg59* prion-inoculated mice did however show a much more subtle form of terminal
317 prion disease. However, based on PrPSc accumulation assessed by western blot or
318 immunohistochemistry and spongiform changes assessed by histopathology, the
319 majority of prion-inoculated *tg59* mice were sacrificed or died around the recorded
320 incubation time for terminal prion disease for this line of mice. This is reflected by the
321 fact that the incubation period for attack rate was similar to that for the incubation
322 period to terminal disease in *tg59* mice. A similar correlation was seen between
323 incubation period for attack rate and incubation period to terminal disease in all of the
324 other mouse lines as shown by the data in Table 1. As a consequence, we consider
325 that prion-inoculated *tg59* mice were culled or died at the terminal stage of prion
326 disease, although they were not initially scored as such according to the criteria of
327 clinical signs described by Dickinson et al, 1968 (28).
328

329 **Lesion profiles of primary passaged scrapie isolates**

330 The brains of mice inoculated with the various scrapie isolates were subjected to
331 neuropathological analysis at terminal prion disease to determine the resultant lesion
332 profile. The data in Figure 2 show the average lesion profile for each scrapie
333 inoculum passaged in conventional or ovine PrP transgenic mice. While the different
334 genotypes of scrapie inocula induced different lesion profiles in each mouse line, the
335 vacuolation patterns were similar between replicate scrapie samples, although this
336 was less so for ARQ/ARQ inocula, especially in *tg59* mice. The greatest degree of
337 similarity between grey matter lesion profiles induced by ARQ/ARQ and VRQ/VRQ
338 inocula was seen in *tg338* mice, Figure 2(e) and 2(j), respectively, where the most
339 apparent difference in pathology score was seen in the thalamic region. In RIII mice,
340 ARQ/ARQ scrapie inocula induced peak pathology scores in the medulla,
341 hypothalamus and septal brain regions with one profile corresponding closely and
342 another with an alternative 1, 4, 7 grey matter pathology score seen for other ARQ
343 inocula upon primary passage in *Prnp*^{a} mice (5). The 1, 4, 7 grey matter lesion profile
344 for ARQ/ARQ inocula passaged in RIII mice was also seen following inoculation of
345 the same samples into *tg338* mice.

346

347 **Genotypic differences in PrPSc distribution in prion-diseased mouse brains**

348 Distinct morphological patterns of PrPSc deposition were evident in the brains of
349 mice that had succumbed to terminal prion disease and differences were evident
350 between PrPSc distribution induced by ARQ/ARQ and VRQ/VRQ scrapie inocula in
351 some lines of mice. A summary of the ovine scrapie-induced PrPSc profile in the
352 various mouse lines is shown in Table 2 and representative photographs are shown

353 in Figure 3. In C57BL/6 mice inoculated with VRQ homozygous scrapie material,
354 widespread particulate PrPSc staining was observed in all coronal sections of the
355 brain examined (frontal cortex, thalamic section, midbrain, medulla and cerebellum).
356 A similar distribution of particulate PrPSc staining was seen in C57BL/6 mice
357 inoculated with ARQ homozygous scrapie material but in addition, amyloid plaques
358 and PrPSc aggregates were also present, most commonly in the thalamus. Similar
359 patterns of PrPSc deposition were also seen in the brains of RIII, VM and *tg59* mice
360 inoculated with either ARQ or VRQ homozygous scrapie isolates, although in *tg59*
361 mice inoculated with VRQ homozygous inocula, the particulate deposition of PrPSc
362 was notably absent in the cerebellar cortex. In contrast to the results seen with all of
363 the other mouse lines, inoculation of *tg338* mice with VRQ/VRQ or ARQ/ARQ scrapie
364 inocula resulted in similar depositions of PrPSc, evident as fine particulate deposits in
365 the hippocampus, thalamus, hypothalamus, midbrain and medulla but not the cortical
366 grey matter of the cerebral and cerebellar cortex or the cerebellar white matter.
367 Significantly, the brains of *tg338* mice inoculated with either genotype of sheep
368 scrapie inocula were characterized by a general absence of amyloid plaques and
369 PrPSc aggregates, commonly seen in all of the other lines of mice that had received
370 the same inocula. There was a low level of intra-neuronal PrPSc deposition in all five
371 mouse lines inoculated with either genotype of scrapie inocula.
372
373 **Quantitation of PrPSc in terminal prion-diseased mouse brains**
374 The distinct patterns of PrPSc deposition in mice inoculated with ARQ/ARQ or
375 VRQ/VRQ scrapie isolates was suggestive of quantitative differences in total PrPSc
376 and its subtypes in the brains of these animals. This was investigated by measuring

377 the level of PrPSc in terminal diseased prion-infected mouse brains using a CDI
378 capable of recognition of PK-sensitive and -resistant disease-associated PrP (63).
379 The capture-detector CDI used anti-PrP monoclonal antibody V24 for capture and
380 monoclonal antibody 6H4 for detection of PrP. In order to quantify disease-
381 associated PrP in the brains of mice with terminal prion disease, PrPSc was
382 extracted by sarkosyl, in the absence or presence of NaPTA precipitation. Native (0
383 M GdnHCl-treated) and denatured (6 M GdnHCl-treated) PrPSc was subsequently
384 quantified by the CDI. Figure 4 shows that significant levels of PrPSc were present in
385 terminal prion-diseased brains of mice inoculated with ARQ or VRQ homozygous
386 scrapie isolates. This was evidenced by the increase in fluorescence counts for
387 sarkosyl-extracted PrPSc treated with 6 M GdnHCl compared to that obtained in the
388 absence of denaturant. In contrast, the level of fluorescence counts for both
389 denatured and native samples obtained from control mice was similar. This reflects
390 the exposure of previously buried epitopes within PrPSc that were no longer
391 accessible in denatured PrPC and confirmed the presence of disease-associated PrP
392 in scrapie isolate-inoculated mice. The level of PrPSc that accumulated in C57BL/6,
393 RIII, VM and *tg59* mice following inoculation with ARQ/ARQ scrapie inocula was
394 significantly greater than that which accumulated after inoculation with VRQ/VRQ
395 inocula ($p<0.001$). In contrast, this trend was reversed in tg338 mice where the level
396 of PrPSc induced by VRQ homozygous scrapie isolates was higher than that induced
397 by ARQ samples, although the differences were not always statistically significant.
398 Similar trends with elevated levels were seen in all mice when PrPSc was quantified
399 following extraction with NaPTA precipitation (data not shown). These qualitative

differences in PrPSc levels measured by CDI correlated with the level of PrPSc described by immunohistochemistry of brain sections from scrapie-inoculated mice.

Molecular profile of ARQ- and VRQ-induced PrPSc and PrP27-30

Different subtypes of PrPSc, distinguished by properties such as PK-resistant fragment length and glycoform ratio, have been associated with different prion strains or with different phenotypes of prion disease in the same species (7, 8, 24, 43, 51, 52, 54, 62). In order to investigate the molecular profile of PrP that arose as a consequence of the primary passage of either ARQ or VRQ homozygous sheep scrapie isolates, mouse brains isolated at terminal prion disease were homogenized and treated with or without PK prior to western blot analysis with anti-PrP monoclonal antibodies. Figure 5 shows that brain homogenates from scrapie-inoculated mice at terminal prion disease contained significant levels of PK-resistant PrPSc in the form of PrP27-30. Brain tissue from scrapie-infected C57BL/6 (Figure 5a), RIII (Figure 5b) and VM mice (data not shown) inoculated with ARQ/ARQ scrapie isolates contained significantly higher levels of total PrP and displayed more PrP27-30 compared to that seen following inoculation with VRQ/VRQ inocula, although the different scrapie isolates were associated with similar incubation times to terminal prion disease in these mice. In contrast, brain tissue from terminal prion-diseased *tg59* (Figure 5c) and *tg338* (Figure 5d) mice inoculated with either ARQ or VRQ sheep scrapie isolates contained similar levels of total PrP and displayed similar levels of PrP27-30. PrPSc induced by either ARQ/ARQ or VRQ/VRQ sheep scrapie isolates was subjected to a titration of PK enzyme in order to determine the susceptibility of PrP27-30 to proteolytic digestion. Despite the significantly different levels of PrP27-

30 generated by PK cleavage of PrPSc in C57BL/6 mouse brains following inoculation with ARQ and VRQ homozygous scrapie isolates, this material showed equal resistance to PK digestion over a wide range of enzyme concentrations (1 – 1000 μg/ml) (data not shown). Similar results were seen when the same titration of PK was used to treat *tg59* and *tg338* prion-infected mouse brain homogenates (data not shown).

Difference in conformational stability of ARQ- and VRQ-induced PrPSc

Prion strains have been characterized by the relative stability of their associated PrPSc, measured by resistance to proteolysis following exposure to GdnHCl (44, 53, 54, 64). Exposure of PrPSc to increasing concentrations of GdnHCl leads to a transition from the native to denatured state, measured as loss of resistance to protease digestion. We have used this approach here to examine the relative stability of PrPSc induced by ARQ and VRQ homozygous scrapie inocula following primary passage in conventional and ovine PrP transgenic mice. Accordingly, aliquots of terminal prion-diseased mouse brain homogenate were incubated with increasing amounts of GdnHCl for 30 min followed by limited proteolysis with PK. The samples were subsequently analyzed by western blot with anti-PrP monoclonal antibody to detect PrP27-30, the protease resistant core of PrPSc. Figure 6 shows that the amount of PrP27-30 detected in PK-treated ARQ- and VRQ-inoculated C57BL/6 mouse brains remained constant following treatment with up to 1.6 M GdnHCl. Exposure to increasing amounts of GdnHCl had little effect on the level of PrP27-30 detected in ARQ-inoculated mice (Figure 6a) but caused an increase in the proteolytic sensitivity of VRQ-induced PrPSc as evidenced by the reduction in PrP27-

448 30 levels on the western blot (Figure 6b). VRQ-induced PrPSc was completely
449 denatured by treatment with >1.6 M GdnHCl (Figure 6b) as evidenced by its
450 complete proteolysis at these concentrations of denaturant. In contrast, significant
451 amounts of PrP27-30 were still evident following treatment of ARQ-induced PrPSc
452 with concentrations of GdnHCl >1.6 M (Figure 6a). These data indicate that VRQ-
453 induced PrPSc in the brains of C57BL/6 mice was more unstable than its ARQ-
454 induced counterpart. Similar trends were seen in *tg59* mice (Figure 6c and 6d), RIII
455 and VM mice (data not shown). In contrast, the amount of PrP27-30 detected in PK-
456 treated ARQ- and VRQ-inoculated *tg338* mouse brains remained constant following
457 treatment with up to 2.0 M GdnHCl, which indicated a similar stability for PrPSc
458 induced by different genotypes of scrapie inocula in this particular mouse line (Figure
459 6e and 6f, respectively). Replicate ARQ and VRQ homozygous sheep scrapie inocula
460 showed similar trends in the stability of denaturant-induced PrPSc following
461 transmission in each of the mouse lines tested (n=3 mouse brains analyzed from
462 each mouse line in which the inoculum was passaged). These data show that the
463 similar levels of PrPSc induced by ARQ/ARQ and VRQ/VRQ scrapie inocula in *tg338*
464 possessed similar denaturant-induced stability, whereas the converse was seen for
465 PrPSc induced by the same inocula in C57BL/6, RIII, VM and *tg59* mice.
466

DISCUSSION

Different isolates of the transmissible scrapie prion agent can exhibit differences in length of incubation period, lesion profile and PrPSc deposition in the brains of affected hosts in which the isolates have been passaged (11, 13, 27, 32). The concept of prion strains has emerged in order to account for this variation in transmission properties exhibited by different scrapie isolates, during serial passage, when variance due to dose, inoculation route, and most importantly, host and donor PrP genotype are taken into account. Historically, ovine prion strain typing has been carried out by serial passage of scrapie isolates in a panel of conventional mice (11). This strategy has allowed a number of different ovine prion strains to be identified and the discrimination between scrapie and BSE (10, 12). However, the failure of some scrapie isolates to transmit to conventional mice is likely to underestimate the true diversity of ovine scrapie strains. Furthermore, passage of ovine prions across a species or transmission barrier may not reveal properties of the infectious prion agent as they exist in the original host. Both of these issues can potentially be circumvented through the use of mice transgenic for ovine PrP. Although facilitated transmission of ovine prions is seen in ovine PrP transgenic mice (4, 26, 43, 69), the utility of these hosts for ovine prion strain typing has not been fully established. Here we have compared the molecular and transmission characteristics of scrapie isolates of different genotypes in ovine PrP transgenic mice and conventional mice in order to begin to address this issue.

The ARQ and VRQ homozygous scrapie isolates used here showed similar glycoform profiles but distinctly different levels of PrP27-30, and presumably therefore different levels of prion infectivity. Despite this, both genotypes of scrapie isolate showed high primary transmission attack rates in C57BL/6, RIII (both *Prnp*^{a}) and VM (*Prnp*^{b}) mouse lines, and *tg59* and *tg338* mice, those transgenic for ovine ARQ or VRQ PrP, respectively. Attack rates for the scrapie isolates in the different mouse lines was in the range of 67 - 100%. Other studies have reported a failure of transmission by some ARQ homozygous isolates in C57BL/6 mice (4, 12). Despite the efficient attack rates seen here for both genotypes of scrapie inocula, similarities and differences in prion disease incubation time were seen between the different prion inoculated mouse lines. Both genotypes of scrapie isolate showed similar primary transmission incubation times in C57BL/6, RIII and VM mice. However, significantly shorter incubation times were seen for all of the scrapie isolates in *tg338* mice. The accelerated rate of prion disease in *tg338* mice may reflect a lower transmission barrier for ovine prion inocula passaged in mice that express ovine PrP compared to that for similar inocula in conventional mouse lines. The fact that a similar level of facilitated transmission was not seen in *tg59* mice may indicate differences in the expression level or location of ovine PrP between the two different ovine PrP transgenic mice. *Tg338* mice express ovine VRQ PrP under the control of the ovine PrP promoter and *tg59* mice express ovine ARQ under the control of the neuron-specific enolase promoter (25, 69). Furthermore, *tg338* mice express approximately 5-fold more ovine PrP protein than do *tg59* mice (our own unpublished observations). However, while *tg338* mice allowed facilitated transmission for both genotypes of scrapie isolates, VRQ/VRQ inocula showed significantly shorter

incubation times in this transgenic mouse line than did ARQ/ARQ inocula. Although the relative susceptibility of *tg338* mice for the ARQ or VRQ homozygous inocula used here could not be assessed because of their potential difference in prion infectivity, as indicated by their different levels of PrP27-30, it was clear that rapid transmission of different genotypes of scrapie inocula occurred in *tg338* mice.

Lesion profiles within terminal prion-diseased ovine PrP transgenic and conventional mouse brains were determined in order to assess the spongiform neurodegeneration induced by transmission of the ARQ/ARQ and VRQ/VRQ inocula. Lesion profiles provide a semi-quantitative assessment of neuropathology in different brain regions, and have been used to discriminate between different prion strains (13, 32, 33). The different lesion profiles reported here for ARQ/ARQ and VRQ/VRQ scrapie inocula are indicative of different prion strains, although the generally distinct neuropathologies resulted from primary transmission of different genotypes of ovine prion inocula. Different strains of the infectious prion agent are revealed, or produced, by passage of prions through hosts of different PrP genotypes (58). To account for this, it is proposed that prion strains comprise an ensemble of PrPSc conformations characterized by a dominant conformer for a given PrP amino acid sequence (22). Accordingly, the ability of prions to replicate within a new host of a different PrP primary amino acid sequence will be influenced by the degree of overlap between the allowed repertoires of PrPSc conformations for both donor and host PrP genotype. In this scheme, passage of prions between hosts occurs more readily when the range of PrPSc conformers overlap but less readily when there is little overlap, with the latter situation leading to the emergence of a new dominant PrPSc conformer or

strain. The propagation of prions between species, or more precisely between different PrP genotypes, may therefore be viewed as a function of thermodynamic stability of PrPSc conformation and the kinetics of its formation and clearance (21, 22). Generally, there was good correlation between lesion profiles induced by replicate ARQ/ARQ or VRQ/VRQ inocula in most of the mouse lines. In addition, lesion profiles for ARQ/ARQ inocula in *tg338* mice were similar to that seen in RIII mice. However, in *tg59* mice somewhat different profiles were obtained during transmission of ARQ/ARQ inocula, which is consistent with selection of different prion strains from the different replicates or the effect of mouse background differences on strain selection. The *tg59* mouse line is produced on a C57BL/6J, 129Sv, and OF1 mixed genetic background (26) and individual mouse variation to particular prion strain susceptibility may occur. Variations in individual genetic backgrounds is considered a possible contributing factor in the apparent selection of different human prion strains following transmission of bovine BSE to mice over-expressing human PrP (3). In contrast to the other mouse lines analyzed here, lesion profiles in *tg338* mice induced by ARQ/ARQ and VRQ/VRQ inocula were very similar, differing most qualitatively in the thalamic grey matter area. This was despite the fact that total PrPSc levels in *tg338* mice measured by CDI following inoculation with ARQ/ARQ or VRQ/VRQ scrapie isolates were fairly similar, whereas in all other mouse lines ARQ/ARQ inocula induced more PrPSc than VRQ/VRQ samples.

We investigated the deposition of PrPSc in the brains of terminal prion-diseased mice by immunohistochemistry. The relatively high levels of total PrPSc in prion-diseased C57BL/6, RIII, VM and *tg59* mouse brains induced by ARQ/ARQ inocula correlated

561 with the presence of aggregated PrP deposition, which was rarely seen in mice that
562 had received VRQ/VRQ inocula. In cases of natural sheep scrapie, there is a
563 genotype-specific differentiation in the pattern and types of disease-associated PrP
564 deposition in the CNS (45, 60). In addition to the PrP genotype of the host, it has
565 been shown that the nature of the inoculum may also significantly affect the pattern of
566 disease-associated PrP deposition (34). Here we have also observed genotype-
567 related differences in the deposition of disease-associated PrP during primary
568 transmissions of ovine scrapie inocula in mice. The increased deposition of PrPSc
569 induced by ARQ/ARQ scrapie isolates seen here in conventional and *tg59* mice may
570 be the result of an increased efficiency in PrPSc formation in these animals. It is
571 worth noting that ovine and murine PrP show significant amino acid homology. Ovine
572 wild type ARQ and VRQ PrP allelic variants differ only in the A→V polymorphism at
573 amino acid position 136 (ovine PrP numbering) and the equivalent amino acid in both
574 *Prnp*^{a} and *Prnp*^{b} genotypes of murine PrP (amino acid residue 133, murine PrP
575 numbering) is an alanine residue (72)**.** Identity at amino acid residue 136 of ovine PrP
576 and at the equivalent amino acid residue in murine PrP may predispose to a more
577 efficient conversion and aggregation of PrPC into PrPSc. Alternatively, the increased
578 deposition of PrPSc aggregates in the brains of mice inoculated with ARQ/ARQ
579 scrapie isolates may suggest that the clearance of PrPSc occurred at a slower rate,
580 or with lower efficiency, than in mice inoculated with VRQ/VRQ isolates. One reason
581 to account for this could be that PrPSc induced by ARQ/ARQ scrapie isolates in
582 *Prnp*^{a}, *Prnp*^{b} and *tg59* mice was more resistant to metabolism than PrPSc that
583 accumulated in similar mice inoculated with VRQ/VRQ scrapie material. This
584 appeared to be the case since ARQ/ARQ-induced PrPSc from these mice was found

585 to be more stable than PrPSc induced by VRQ/VRQ inocula. Studies of prion proteins
586 in other biological systems, such as yeast, have suggested that the strain-specific
587 properties correlate with the physical properties of prion protein aggregates, such as
588 frangibility, which may contribute to their metabolic fate (61).
589
590 It has been a long-standing assumption that PrPSc is primarily responsible for
591 spongiform neurodegeneration in prion diseases because of the correlation between
592 its anatomical and temporal accumulation and the ensuing neuropathology. The fact
593 that different levels of PrPSc accumulate in the brains of mice that succumbed to
594 terminal prion disease with similar incubation times suggests that the level of PrPSc
595 measured here does not directly correlate with the extent of pathology or
596 neurotoxicity. Conversion of PrPC to PrPSc is a fundamental feature of prion disease
597 pathogenesis since PrP-/- mice are resistant to prion infection (15, 48). However, the
598 mechanism of neurotoxicity remains to be elucidated (19). While it is established that
599 neurons must express PrPC to be susceptible to toxicity there are several examples
600 of prion disease or experimental transmissions where the levels of PrPSc are low or
601 apparently absent (23, 36, 42, 49, 50). In contrast, high levels of PrPSc may
602 accumulate in the absence of full-blown clinical disease (35, 56, 65, 66). In addition,
603 ablation of neuronal PrPC expression during on-going prion disease in mice can
604 prevent the onset of clinical signs and reverse early spongiform neuropathology (46,
605 47). An emerging view is that large aggregated forms of PrPSc are relatively inert
606 and innocuous, and smaller, potentially labile, oligomeric species of PrP generated
607 as an intermediate during prion replication constitute the actual neurotoxic agent (2,
608 14, 20, 35, 70). According to this scheme, a critical level of neurotoxic PrP must

609 accumulate in order for the prion-infected individual to develop spongiform
610 neurodegeneration. In the context of the protein-only hypothesis, the relatively long
611 incubation times seen for sheep scrapie inocula in conventional mice can be
612 interpreted as the result of an inefficient conversion of PrPC to PrPSc across the
613 sheep – mouse species barrier, with a corresponding slow accumulation of the
614 neurotoxic form of PrP. In contrast, the short incubation times for sheep scrapie
615 inocula in *tg338* mice can be seen to occur as a result of their high level of ovine
616 PrPC expression, leading to an efficient conversion of PrP coupled with fast
617 accumulation of the neurotoxic PrP intermediate.
618
619 Although *tg338* mice showed short incubation periods for the onset of terminal prion
620 disease following inoculation with sheep scrapie isolates, these mice displayed a
621 more uniform phenotype with regards to those parameters typically used to
622 distinguish different ovine prion strains. Scrapie-inoculated *tg338* mice showed
623 similar lesion profiles that were accompanied by similar PrPSc depositions following
624 inoculation with either ARQ or VRQ homozygous scrapie isolates, whereas different
625 patterns were seen in similarly inoculated *tg59* and conventional mouse lines. These
626 observations imply that *tg338* mice may reveal a different range of ovine prion strains
627 than do *tg59* mice and that *tg59* mice may more closely resemble conventional mice
628 in the range of ovine prion strains that they can replicate. This difference between
629 *tg338* and *tg59* mice in their potential to distinguish or generate ovine prion strains
630 also correlates with the conformational variation of PrPSc that accumulates in these
631 VRQ and ARQ ovine PrP transgenic mice. PrPSc that accumulated in ARQ *tg59*
632 mice showed different denaturant-induced stability following inoculation with either

ARQ or VRQ homozygous inocula whereas PrPSc that accumulated in similarly inoculated *tg338* mice showed similar stability. We, and others, have previously shown that ovine VRQ PrP is more stable than ovine ARQ PrP (16, 29, 57) and this may reflect that ovine PrP with alanine at amino acid residue 136 is more flexible in its ability to adopt different conformations than is ovine PrP with valine at amino acid residue 136. This would in turn suggest that host PrP genotype plays a dominant role in distinguishing or generating ovine prion strains. Differences in prion disease phenotype were observed in the ovine PrP transgenic mouse lines after inoculation with scrapie isolates from sheep of different PrP genotypes. Whether these differences represent stable variations, and hence strain variation, can only be confirmed by further serial passage. If strain differences are confirmed, this would suggest that these transgenic lines may allow for a stable strain phenotype to be observed on first passage. This would be a significant advantage for the use of ovine PrP transgenic animals in ovine prion strain typing. Subsequent serial passage in *tg338*, *tg59* and conventional mice of the different scrapie isolates used here will be required in order to determine the validity of this approach and these studies are currently underway.

657 **ACKNOWLEDGEMENTS**

658

659 This work was supported by funds from Defra. LH is in receipt of a Defra PhD
660 studentship. We thank INRA Jouy-en-Josas for supply of the *tg338* mouse line. We
661 thank Thierry Baron for supply of the *tg59* mouse line. We thank support staff in the
662 Departments of Histology, Neuropathology and the Animal Services Unit of the VLA,
663 Weybridge for their skilled sample preparation and handling.

664

664 **LEGENDS**

665

666 **Figure 1. Western blot analysis of ARQ/ARQ and VRQ/VRQ ovine scrapie**
667 **isolates**

668 Homogenates of ARQ/ARQ and VRQ/VRQ ovine scrapie isolates were prepared as
669 described in the Materials and Methods and analyzed by SDS-PAGE and western
670 blot using anti-PrP monoclonal antibody P4 at 1 μg/ml. Upper panel: Homogenates
671 were treated with or without various concentrations of PK. Lower panel: Tracks 1 – 4:
672 10% homogenate; track 5: 5% homogenate; track 6: 2.5% homogenate; tracks 1 and
673 3: no PK; tracks 2, 4 – 6: PK at 32 μg/ml. Molecular mass markers (kDa) are shown
674 on the left.

675

676 **Table 1. Primary passage incubation times for sheep scrapie inocula in**
677 **conventional and ovine PrP transgenic mice**

678 Mice were inoculated with ARQ/ARQ and VRQ/VRQ sheep scrapie isolates by a
679 combined intra-cranial and intra-peritoneal route. Inoculated mice were monitored for
680 clinical signs of mouse prion disease. Mice scored positive for terminal prion disease
681 were those that displayed clinical signs for this condition as described by Dickinson
682 et al, 1968 (28). The majority of prion-inoculated *tg59* mice showed a much more
683 subtle form of terminal prion disease. Mice were euthanized at the point of
684 neurological disease and dysfunction and prion disease confirmed by histopathology,
685 immunohistochemistry for disease-associated PrP or western blot for PK-resistant
686 PrP27-30. The data shown are incubation times for terminal prion disease and attack
687 rate. Incubation time for terminal prion disease was calculated as the time from

688 inoculation to euthanazia at terminal prion disease ± SD; figures in parenthesis are
689 numbers of terminal prion diseased mice / total number of mice positive for prion
690 disease, for that group. Incubation time for attack rate was calculated as the time
691 from inoculation to death or euthanazia (for whatever reason) for prion-diseased-
692 positive mice ± SD; figures in parenthesis are numbers of prion-diseased-positive
693 mice / the number surviving after, and including, the first positive diagnosis, for that
694 group. NA = not available. Statistical analysis of the data was performed by one-way
695 ANOVA together with Tukey HSD (honestly significant difference) for *post hoc*
696 analysis.
697 a = $p \leq 0.01$ in comparison with VM mice
698 b = $p \leq 0.05$ in comparison with C57BL/6 mice
699 c = $p < 0.001$ in comparison with C57BL/6 and RIII mice
700 d = $p < 0.001$ in comparison with C57BL/6, RIII and VM mice
701 e = $p < 0.001$ in comparison with *tg338* mice inoculated with the VRQ scrapie isolates
702 f = $p < 0.001$ in comparison with C57BL/6 and VM mice
703 g = $p < 0.001$ in comparison with *tg59* mice
704 h = $p < 0.01$ in comparison with *tg338* mice inoculated with the VRQ scrapie isolates
705
706 **Figure 2. Lesion profiles induced by primary transmissions of ovine scrapie**
707 **isolates**
708 Prion-infected brains were harvested from mice that had developed terminal prion
709 disease and were subjected to neuropathological examination for the presence and
710 severity of spongiform neurodegeneration. The lesion profiles shown are (a) and (f)

C57BL/6; (b) and (g) RIII; (c) and (h) VM; (d) and (i) *tg59* and (e) and (j) *tg338* mice inoculated with ARQ/ARQ (a) – (e) or VRQ/VRQ (f) – (j) sheep scrapie isolates. Lesion profiles induced by: thick line (a) – (e), SE1848/0007 (ARQ/ARQ); dashed line (a) – (e), SE1848/0008 (ARQ/ARQ); thick line (f) – (j), SE1848/0005 (VRQ/VRQ); dashed line (f) – (j), SE1848/0006 (VRQ/VRQ). The data shown are mean lesion profile scores (n≥3 brains examined) for the following brain areas: grey (G) matter, G1: dorsal medulla nuclei; G2: cerebellar cortex of the folia including the granular layer, adjacent to the fourth ventricle; G3: cortex of the superior colliculus; G4: hypothalamus; G5: thalamus; G6: hippocampus; G7: septal nuclei of the paraterminal body; G8: cerebral cortex (at the level of G4 and G5); G9: cerebral cortex (at the level of G7) or white (W) matter, W1: cerebellar peduncles; W2: white matter in lateral tegmentum; W3: cerebellar peduncle / internal capsule. No data was obtainable for SE1848/0007 in VM mice (c).

Table 2. Disease-associated PrP distribution in the brains of mice with terminal prion disease

Immunohistochemistry summary of particulate and aggregated PrPSc in the brains of prion-infected mouse brains. +: present in all mice; -:absent in all mice; +/-: present in the majority of mice; -/+: present in a minority of mice.

Figure 3. Immunohistochemistry of prion-infected mouse brains

A and B: PrPSc patterns in the cortex and hippocampus of C57BL/6 mice inoculated with ovine ARQ/ARQ and VRQ/VRQ 'good' transmitter isolates, respectively. Granular deposits were evident in both cases but aggregates and plaques were

735 observed only in the mice inoculated with ARQ/ARQ isolates. C: PrPSc patterns in
736 the thalamus of *tg59* mice inoculated with ARQ/ARQ scrapie isolates showing
737 granular PrPSc deposits and larger aggregates distributed throughout the thalamic
738 region. D: Granular PrPSc patterns in the hypothalamus of *tg59* mice inoculated with
739 ARQ/ARQ scrapie isolates. Large aggregates and plaques were also evident in the
740 ventral thalamus. Plaques were the predominant PrPSc deposits in the ventral
741 thalamus while only rarely were small granular PrPSc deposits observed in the rest of
742 the thalamic region. E: PrPSc patterns in the thalamus of *tg59* mice inoculated with
743 VRQ/VRQ isolates showing granular PrPSc. Aggregates and plaques were observed
744 only in the mice inoculated with ARQ/ARQ isolates. F and G: PrPSc patterns in the
745 cortex, hippocampus, thalamus and dorsal hypothalamus of *tg338* mice inoculated
746 with ARQ/ARQ and VRQ/VRQ scrapie isolates respectively. Fine granular deposits,
747 not obvious at this magnification, were evident in both cases but aggregates of PrPSc
748 along the corpus calosum were only observed in the mice inoculated with ARQ/ARQ
749 isolates. H: High magnification of the hypothalamus from the same *tg338* animal as
750 in picture G to demonstrate PrPSc deposits located in the neuron, glial cells and
751 neuropil. Scale bar: in A-I 500µm; in F 50µm.
752
753 **Figure 4. Relative levels of total PrPSc in prion-infected mouse brains**
754 **measured by CDI**
755 Prion-infected brains were harvested from mice that had developed terminal prion
756 disease and homogenates were prepared in sarkosyl as described in the Materials
757 and Methods. Native (0 M-treated) and denatured (6 M-treated) PrPSc was captured
758 by anti-PrP monoclonal antibody V24 and detected by biotinylated anti-PrP

759 monoclonal antibody 6H4 followed by Europium-labeled streptavidin. The data shown
760 are the mean time-resolved fluorescence counts per second (cps) ± SD for each
761 treatment group. (a) C57BL/6; (b) VM; (c) *tg59*; (d) *tg338*. White bar: 0 M GdnHCl;
762 Black bar: 6 M GdnHCl. Statistical analysis of the data, with *p* values shown in the
763 text, was performed using the two-tailed Student *t* test (unpaired samples).
764
765 **Figure 5. Western blot detection of PrP**
766 Prion-infected brains were harvested from mice that had developed terminal prion
767 disease and homogenates were prepared as described in the Materials and
768 Methods. Brain homogenates were treated with or without PK and analyzed by SDS-
769 PAGE and western blot with anti-PrP monoclonal antibody 683 for (a) C57BL/6; (b)
770 RIII mouse brains and monoclonal antibody P4 for (c) *tg59*; (d) *tg338* mouse brains.
771 Each track was loaded with 25 μg of total protein. Molecular mass markers (kDa) are
772 shown on the left.
773
774 **Figure 6. Conformational stability of ARQ- and VRQ-induced PrPSc**
775 Prion-infected mouse brain homogenates were prepared as described in the
776 Materials and Methods. Brain homogenates were treated with or without GdnHCl at
777 final concentrations as shown followed by incubation in the presence or absence of
778 PK and subsequently analyzed by SDS-PAGE and western blot with anti-PrP
779 monoclonal antibody 683 (a) and (b); or monoclonal antibody P4 (c) - (f). The western
780 blots show PrP from C57BL/6 mice (a) and (b); *tg59* mice (c) and (d); or *tg338* mice
781 (e) and (f). Mice were inoculated with ARQ/ARQ (a), (c) and (e); or VRQ/VRQ (b), (d)
782 and (f) sheep scrapie isolates. Molecular mass markers (kDa) are shown on the left.

REFERENCES

1. **Aguzzi, A., M. Heikenwalder, and M. Polymenidou.** 2007. Insights into prion strains and neurotoxicity. Nat. Rev. Mol. Cell Biol. **8:**552-561.
2. **Anderson, M., O. V. Bocharova, N. Makarava, L. Breydo, V. V. Salnikov, and I. V. Baskakov.** 2006. Polymorphism and ultrastructural organization of prion protein amyloid fibrils: an insight from high resolution atomic force microscopy. J. Mol. Biol. **358:**580-596.
3. **Asante, E. A., J. M. Linehan, M. Desbruslais, S. Joiner, I. Gowland, A. L. Wood, J. Welch, A. F. Hill, S. E. Lloyd, J. D. Wadsworth, and J. Collinge.** 2002. BSE prions propagate as either variant CJD-like or sporadic CJD-like prion strains in transgenic mice expressing human prion protein. EMBO J. **21:**6358-6366.
4. **Baron, T., C. Crozet, A. G. Biacabe, S. Philippe, J. Verchere, A. Bencsik, J. Y. Madec, D. Calavas, and J. Samarut.** 2004. Molecular analysis of the protease-resistant prion protein in scrapie and bovine spongiform encephalopathy transmitted to ovine transgenic and wild-type mice. J. Virol. **78:**6243-6251.
5. **Beck, K., R. Salis, S. Simonini, and J. Spiropoulos.** 2007. Primary isolation of the scrapie agent in RIII mice: identification of sheep PrP genotype-associated profiles. Prion 2007: European Network of Excellence Neuroprion. 2007; Abstract P02.20.
6. **Beringue, V., A. Bencsik, A. Le Dur, F. Reine, T. L. Lai, N. Chenais, G. Tilly, A. G. Biacabe, T. Baron, J. L. Vilotte, and H. Laude.** 2006. Isolation

from cattle of a prion strain distinct from that causing bovine spongiform encephalopathy. PLoS Pathog. **2:**e112.

7. **Bessen, R. A., and R. F. Marsh.** 1992. Biochemical and physical properties of the prion protein from two strains of the transmissible mink encephalopathy agent. J. Virol. **66:**2096-2101.

8. **Bessen, R. A., and R. F. Marsh.** 1994. Distinct PrP properties suggest the molecular basis of strain variation in transmissible mink encephalopathy. J. Virol. **68:**7859-7868.

9. **Browning, S. R., G. L. Mason, T. Seward, M. Green, G. A. Eliason, C. Mathiason, M. W. Miller, E. S. Williams, E. Hoover, and G. C. Telling.** 2004. Transmission of prions from mule deer and elk with chronic wasting disease to transgenic mice expressing cervid PrP. J. Virol. **78:**13345-13350.

10. **Bruce, M. E.** 1993. Scrapie strain variation and mutation. Br. Med. Bull. **49:**822-838.

11. **Bruce, M. E.** 2003. TSE strain variation. Br. Med. Bull. **66:**99-108.

12. **Bruce, M. E., A. Boyle, S. Cousens, I. McConnell, J. Foster, W. Goldmann, and H. Fraser.** 2002. Strain characterization of natural sheep scrapie and comparison with BSE. J. Gen. Virol. **83:**695-704.

13. **Bruce, M. E., and H. Fraser.** 1991. Scrapie strain variation and its implications. Curr. Top. Microbiol. Immunol. **172:**125-138.

14. **Bucciantini, M., E. Giannoni, F. Chiti, F. Baroni, L. Formigli, J. Zurdo, N. Taddei, G. Ramponi, C. M. Dobson, and M. Stefani.** 2002. Inherent toxicity of aggregates implies a common mechanism for protein misfolding diseases. Nature **416:**507-511.

15. **Bueler, H., A. Aguzzi, A. Sailer, R. A. Greiner, P. Autenried, M. Aguet, and C. Weissmann.** 1993. Mice devoid of PrP are resistant to scrapie. Cell **73:**1339-1347.

16. **Bujdoso, R., D. F. Burke, and A. M. Thackray.** 2005. Structural differences between allelic variants of the ovine prion protein revealed by molecular dynamics simulations. Proteins **61:**840-849.

17. **Buschmann, A., E. Pfaff, K. Reifenberg, H. M. Muller, and M. H. Groschup.** 2000. Detection of cattle-derived BSE prions using transgenic mice overexpressing bovine PrP(C). Arch. Virol. Supplement**:**75-86.

18. **Chesebro, B.** 1998. BSE and prions: uncertainties about the agent. Science **279:**42-43.

19. **Chiesa, R., and D. A. Harris.** 2001. Prion diseases: what is the neurotoxic molecule? Neurobiol. Dis. **8:**743-763.

20. **Chiesa, R., P. Piccardo, E. Quaglio, B. Drisaldi, S. L. Si-Hoe, M. Takao, B. Ghetti, and D. A. Harris.** 2003. Molecular distinction between pathogenic and infectious properties of the prion protein. J. Virol. **77:**7611-7622.

21. **Collinge, J.** 1999. Variant Creutzfeldt-Jakob disease. Lancet **354:**317-323.

22. **Collinge, J., and A. R. Clarke.** 2007. A general model of prion strains and their pathogenicity. Science **318:**930-936.

23. **Collinge, J., M. S. Palmer, K. C. Sidle, I. Gowland, R. Medori, J. Ironside, and P. Lantos.** 1995. Transmission of fatal familial insomnia to laboratory animals. Lancet **346:**569-570.

24. **Collinge, J., K. C. Sidle, J. Meads, J. Ironside, and A. F. Hill.** 1996. Molecular analysis of prion strain variation and the aetiology of 'new variant' CJD. Nature **383:**685-690.

25. **Cordier, C., A. Bencsik, S. Philippe, D. Betemps, F. Ronzon, D. Calavas, C. Crozet, and T. Baron.** 2006. Transmission and characterization of bovine spongiform encephalopathy sources in two ovine transgenic mouse lines (TgOvPrP4 and TgOvPrP59). J. Gen. Virol. **87:**3763-3771.

26. **Crozet, C., F. Flamant, A. Bencsik, D. Aubert, J. Samarut, and T. Baron.** 2001. Efficient transmission of two different sheep scrapie isolates in transgenic mice expressing the ovine PrP gene. J. Virol. **75:**5328-5334.

27. **Dickinson, A. G., and V. M. Meikle.** 1971. Host-genotype and agent effects in scrapie incubation: change in allelic interaction with different strains of agent. Mol. Gen. Genet. **112:**73-79.

28. **Dickinson, A. G., V. M. Meikle, and H. Fraser.** 1968. Identification of a gene which controls the incubation period of some strains of scrapie agent in mice. J. Comp. Pathol. **78:**293-299.

29. **Eghiaian, F., J. Grosclaude, S. Lesceu, P. Debey, B. Doublet, E. Treguer, H. Rezaei, and M. Knossow.** 2004. Insight into the PrPC-->PrPSc conversion from the structures of antibody-bound ovine prion scrapie-susceptibility variants. Proc. Natl. Acad. Sci. USA **101:**10254-10259.

30. **Espinosa, J. C., O. Andreoletti, J. Castilla, M. E. Herva, M. Morales, E. Alamillo, F. D. San-Segundo, C. Lacroux, S. Lugan, F. J. Salguero, J. Langeveld, and J. M. Torres.** 2007. Sheep-passaged bovine spongiform

876 encephalopathy agent exhibits altered pathobiological properties in bovine-PrP
877 transgenic mice. J. Virol. **81:**835-843.
878 31. **Farquhar, C. F., R. A. Somerville, and M. E. Bruce.** 1998. Straining the
879 prion hypothesis. Nature **391:**345-346.
880 32. **Fraser, H., and A. G. Dickinson.** 1973. Scrapie in mice. Agent-strain
881 differences in the distribution and intensity of grey matter vacuolation. J.
882 Comp. Pathol. **83:**29-40.
883 33. **Fraser, H., and A. G. Dickinson.** 1968. The sequential development of the
884 brain lesion of scrapie in three strains of mice. J. Comp. Pathol. **78:**301-311.
885 34. **Gonzalez, L., S. Martin, I. Begara-McGorum, N. Hunter, F. Houston, M.**
886 **Simmons, and M. Jeffrey.** 2002. Effects of agent strain and host genotype on
887 PrP accumulation in the brain of sheep naturally and experimentally affected
888 with scrapie. J. Comp. Pathol. **126:**17-29.
889 35. **Hill, A. F., S. Joiner, J. Linehan, M. Desbruslais, P. L. Lantos, and J.**
890 **Collinge.** 2000. Species-barrier-independent prion replication in apparently
891 resistant species. Proc. Natl. Acad. Sci. USA **97:**10248-10253.
892 36. **Hsiao, K. K., M. Scott, D. Foster, D. F. Groth, S. J. DeArmond, and S. B.**
893 **Prusiner.** 1990. Spontaneous neurodegeneration in transgenic mice with
894 mutant prion protein. Science **250:**1587-1590.
895 37. http://www.defra.gov.uk/corporate/vla/science/documents/science-tse-rl-prp-
896 ihc.pdf**.**
897 38. **Kimberlin, R. H., S. Cole, and C. A. Walker.** 1987. Temporary and
898 permanent modifications to a single strain of mouse scrapie on transmission to
899 rats and hamsters. J. Gen. Virol. **68:**1875-1881.

39. **Kimberlin, R. H., and C. A. Walker.** 1978. Evidence that the transmission of one source of scrapie agent to hamsters involves separation of agent strains from a mixture. J. Gen. Virol. **39:**487-496.

40. **Kimberlin, R. H., C. A. Walker, and H. Fraser.** 1989. The genomic identity of different strains of mouse scrapie is expressed in hamsters and preserved on reisolation in mice. J. Gen. Virol. **70:**2017-2025.

41. **Korth, C., B. Stierli, P. Streit, M. Moser, O. Schaller, R. Fischer, W. Schulz-Schaeffer, H. Kretzschmar, A. Raeber, U. Braun, F. Ehrensperger, S. Hornemann, R. Glockshuber, R. Riek, M. Billeter, K. Wuthrich, and B. Oesch.** 1997. Prion (PrPSc)-specific epitope defined by a monoclonal antibody. Nature **390:**74-77.

42. **Lasmezas, C. I., J. P. Deslys, O. Robain, A. Jaegly, V. Beringue, J. M. Peyrin, J. G. Fournier, J. J. Hauw, J. Rossier, and D. Dormont.** 1997. Transmission of the BSE agent to mice in the absence of detectable abnormal prion protein. Science **275:**402-405.

43. **Le Dur, A., V. Beringue, O. Andreoletti, F. Reine, T. L. Lai, T. Baron, B. Bratberg, J. L. Vilotte, P. Sarradin, S. L. Benestad, and H. Laude.** 2005. A newly identified type of scrapie agent can naturally infect sheep with resistant PrP genotypes. Proc. Natl. Acad. Sci. USA **102:**16031-16036.

44. **Legname, G., H. O. Nguyen, D. Peretz, F. E. Cohen, S. J. DeArmond, and S. B. Prusiner.** 2006. Continuum of prion protein structures enciphers a multitude of prion isolate-specified phenotypes. Proc. Natl. Acad. Sci. USA **103:**19105-19110.

45. **Ligios, C., G. Dexter, J. Spiropoulos, C. Maestrale, A. Carta, and M. M. Simmons.** 2004. Distribution of vascular amyloid in scrapie-affected sheep with different genotypes. J. Comp. Pathol. **131:**271-276.

46. **Mallucci, G., A. Dickinson, J. Linehan, P. C. Klohn, S. Brandner, and J. Collinge.** 2003. Depleting neuronal PrP in prion infection prevents disease and reverses spongiosis. Science **302:**871-874.

47. **Mallucci, G. R., M. D. White, M. Farmer, A. Dickinson, H. Khatun, A. D. Powell, S. Brandner, J. G. Jefferys, and J. Collinge.** 2007. Targeting cellular prion protein reverses early cognitive deficits and neurophysiological dysfunction in prion-infected mice. Neuron **53:**325-335.

48. **Manson, J. C., A. R. Clarke, P. A. McBride, I. McConnell, and J. Hope.** 1994. PrP gene dosage determines the timing but not the final intensity or distribution of lesions in scrapie pathology. Neurodegeneration **3:**331-340.

49. **Manson, J. C., E. Jamieson, H. Baybutt, N. L. Tuzi, R. Barron, I. McConnell, R. Somerville, J. Ironside, R. Will, M. S. Sy, D. W. Melton, J. Hope, and C. Bostock.** 1999. A single amino acid alteration (101L) introduced into murine PrP dramatically alters incubation time of transmissible spongiform encephalopathy. EMBO J. **18:**6855-6864.

50. **Medori, R., P. Montagna, H. J. Tritschler, A. LeBlanc, P. Cortelli, P. Tinuper, E. Lugaresi, and P. Gambetti.** 1992. Fatal familial insomnia: a second kindred with mutation of prion protein gene at codon 178. Neurology **42:**669-670.

51. **Monari, L., S. G. Chen, P. Brown, P. Parchi, R. B. Petersen, J. Mikol, F. Gray, P. Cortelli, P. Montagna, B. Ghetti, and et al.** 1994. Fatal familial

insomnia and familial Creutzfeldt-Jakob disease: different prion proteins determined by a DNA polymorphism. Proc. Natl. Acad. Sci. USA **91:**2839-2842.

52. **Parchi, P., R. Castellani, S. Capellari, B. Ghetti, K. Young, S. G. Chen, M. Farlow, D. W. Dickson, A. A. Sima, J. Q. Trojanowski, R. B. Petersen, and P. Gambetti.** 1996. Molecular basis of phenotypic variability in sporadic Creutzfeldt-Jakob disease. Ann. Neurol. **39:**767-778.

53. **Peretz, D., M. R. Scott, D. Groth, R. A. Williamson, D. R. Burton, F. E. Cohen, and S. B. Prusiner.** 2001. Strain-specified relative conformational stability of the scrapie prion protein. Protein Sci. **10:**854-863.

54. **Peretz, D., R. A. Williamson, G. Legname, Y. Matsunaga, J. Vergara, D. R. Burton, S. J. DeArmond, S. B. Prusiner, and M. R. Scott.** 2002. A change in the conformation of prions accompanies the emergence of a new prion strain. Neuron **34:**921-932.

55. **Prusiner, S. B.** 1982. Novel proteinaceous infectious particles cause scrapie. Science **216:**136-144.

56. **Race, R., A. Raines, G. J. Raymond, B. Caughey, and B. Chesebro.** 2001. Long-term subclinical carrier state precedes scrapie replication and adaptation in a resistant species: analogies to bovine spongiform encephalopathy and variant Creutzfeldt-Jakob disease in humans. J. Virol. **75:**10106-10112.

57. **Rezaei, H., Y. Choiset, F. Eghiaian, E. Treguer, P. Mentre, P. Debey, J. Grosclaude, and T. Haertle.** 2002. Amyloidogenic unfolding intermediates differentiate sheep prion protein variants. J. Mol. Biol. **322:**799-814.

58. **Ridley, R. M., and H. F. Baker.** 1996. To what extent is strain variation evidence for an independent genome in the agent of the transmissible spongiform encephalopathies? Neurodegeneration **5:**219-231.

59. **Safar, J., H. Wille, V. Itri, D. Groth, H. Serban, M. Torchia, F. E. Cohen, and S. B. Prusiner.** 1998. Eight prion strains have PrP(Sc) molecules with different conformations. Nat. Med. **4:**1157-1165.

60. **Spiropoulos, J., C. Casalone, M. Caramelli, and M. M. Simmons.** 2007. Immunohistochemistry for PrPSc in natural scrapie reveals patterns which are associated with the PrP genotype. Neuropathol. Appl. Neurobiol. **33:**398-409.

61. **Tanaka, M., S. R. Collins, B. H. Toyama, and J. S. Weissman.** 2006. The physical basis of how prion conformations determine strain phenotypes. Nature **442:**585-589.

62. **Telling, G. C., P. Parchi, S. J. DeArmond, P. Cortelli, P. Montagna, R. Gabizon, J. Mastrianni, E. Lugaresi, P. Gambetti, and S. B. Prusiner.** 1996. Evidence for the conformation of the pathologic isoform of the prion protein enciphering and propagating prion diversity. Science **274:**2079-2082.

63. **Thackray, A. M., L. Hopkins, and R. Bujdoso.** 2007. Proteinase K-sensitive disease-associated ovine prion protein revealed by conformation-dependent immunoassay. Biochem. J. **401:**475-483.

64. **Thackray, A. M., L. Hopkins, M. A. Klein, and R. Bujdoso.** 2007. Mouse-adapted ovine scrapie prion strains are characterized by different conformers of PrPSc. J. Virol. **81:**12119-12127.

65. **Thackray, A. M., M. A. Klein, A. Aguzzi, and R. Bujdoso.** 2002. Chronic subclinical prion disease induced by low-dose inoculum. J. Virol. **76:**2510-2517.

66. **Thackray, A. M., M. A. Klein, and R. Bujdoso.** 2003. Subclinical prion disease induced by oral inoculation. J. Virol. **77:**7991-7998.

67. **Thackray, A. M., S. Yang, E. Wong, T. J. Fitzmaurice, R. J. Morgan-Warren, and R. Bujdoso.** 2004. Conformational variation between allelic variants of cell-surface ovine prion protein. Biochem. J. **381:**221-229.

68. **Thuring, C. M., J. H. Erkens, J. G. Jacobs, A. Bossers, L. J. Van Keulen, G. J. Garssen, F. G. Van Zijderveld, S. J. Ryder, M. H. Groschup, T. Sweeney, and J. P. Langeveld.** 2004. Discrimination between scrapie and bovine spongiform encephalopathy in sheep by molecular size, immunoreactivity, and glycoprofile of prion protein. J. Clin. Microbiol. **42:**972-980.

69. **Vilotte, J. L., S. Soulier, R. Essalmani, M. G. Stinnakre, D. Vaiman, L. Lepourry, J. C. Da Silva, N. Besnard, M. Dawson, A. Buschmann, M. Groschup, S. Petit, M. F. Madelaine, S. Rakatobe, A. Le Dur, D. Vilette, and H. Laude.** 2001. Markedly increased susceptibility to natural sheep scrapie of transgenic mice expressing ovine prp. J. Virol. **75:**5977-5984.

70. **Walsh, D. M., I. Klyubin, J. V. Fadeeva, W. K. Cullen, R. Anwyl, M. S. Wolfe, M. J. Rowan, and D. J. Selkoe.** 2002. Naturally secreted oligomers of amyloid beta protein potently inhibit hippocampal long-term potentiation in vivo. Nature **416:**535-539.

71. **Weissmann, C.** 1991. A 'unified theory' of prion propagation. Nature **352:**679-683.

72. **Wopfner, F., G. Weidenhofer, R. Schneider, A. von Brunn, S. Gilch, T. F. Schwarz, T. Werner, and H. M. Schatzl.** 1999. Analysis of 27 mammalian and 9 avian PrPs reveals high conservation of flexible regions of the prion protein. J. Mol. Biol. **289:**1163-1178.

Figure 1. Western blot analysis of ARQ/ARQ and VRQ/VRQ ovine scrapie isolates

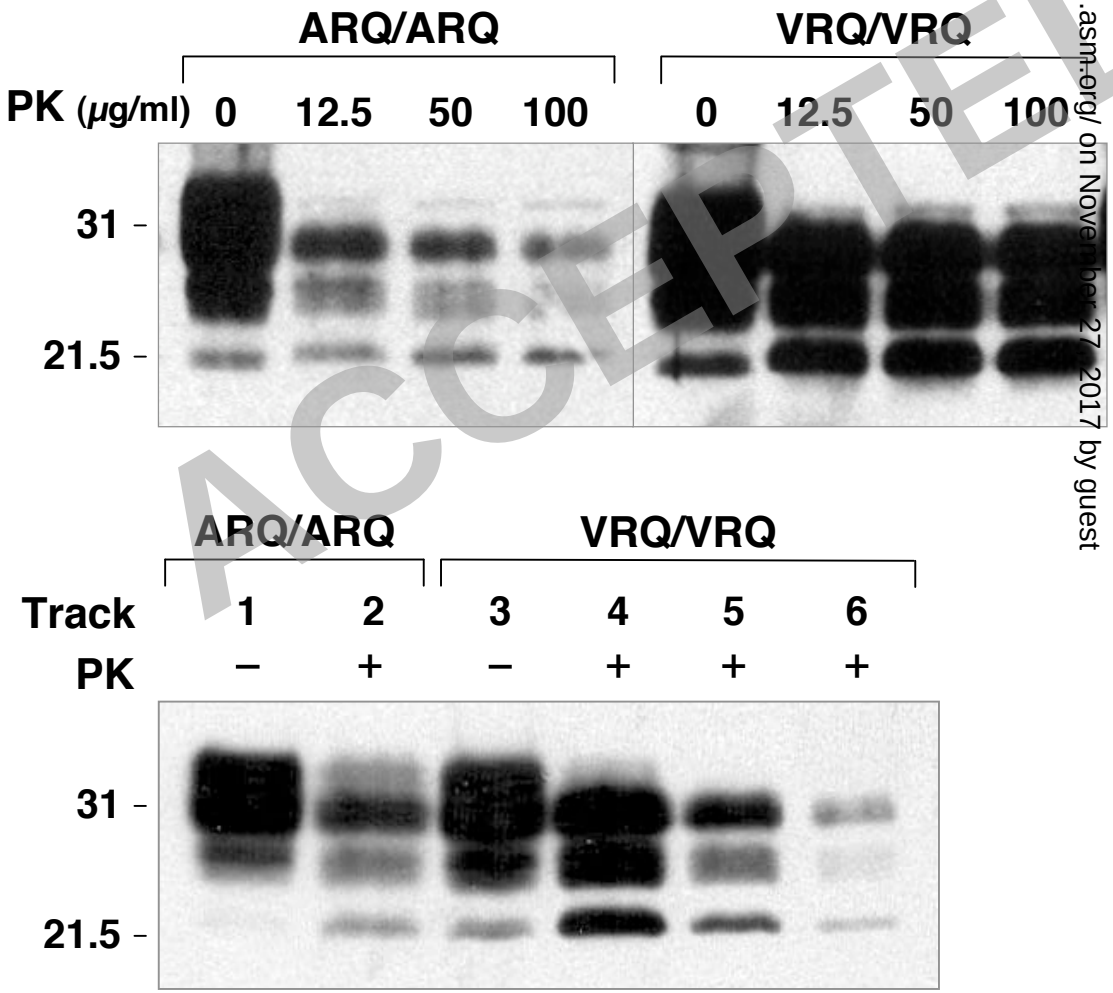

Table 1. Primary passage data for sheep scrapie inocula

Sample	Incubation time	C57BL/6	RIII	VM	*tg59*	*tg338*
ARQ SE1848 0007	Terminal disease	468 ± 16 (16/16)	458 ± 6 [a] (3/4)	617 ± 8 [b] (3/12)	NA (0/16)	210 ± 197 [d, e] (5/14)
	Attack rate	468 ± 16 (16/16)	450 ± 17 (4/4)	586 ± 54 [b] (12/14)	470 ± 56 [a] (16/16)	318 ± 235 [e, f, g] (14/14)
ARQ SE1848 0008	Terminal disease	395 ± 50 (14/15)	422 ± 11 (12/14)	565 ± 30 [c] (12/17)	392 ± 50 (2/14)	155 ± 4 [d, h] (12/12)
	Attack rate	387 ± 56 (15/15)	398 ± 52 (14/15)	565 ± 34 [c] (17/17)	331 ± 61 [a] (14/14)	155 ± 4 [d, g] (12/13)
VRQ SE1848 0005	Terminal disease	549 ± 43 (15/16)	487 ± 28 [b] (13/15)	551 ± 61 (14/17)	434 ± 0 (1/14)	64 ± 2 [d] (16/16)
	Attack rate	548 ± 42 (16/16)	486 ± 28 (15/16)	557 ± 76 (17/19)	440 ± 60 [a, b] (14/14)	64 ± 2 [d, g] (16/16)
VRQ SE1848 0006	Terminal disease	527 ± 49 (13/13)	492 ± 23 (8/10)	524 ± 59 (9/12)	403 ± 0 (1/12)	63 ± 1 [d] (13/15)
	Attack rate	527 ± 49 (13/13)	489 ± 24 (10/10)	526 ± 66 (12/18)	460 ± 57 (12/12)	63 ± 1 [d, g] (15/15)

Figure 2. Lesion profiles induced by primary transmissions of ovine scrapie isolates

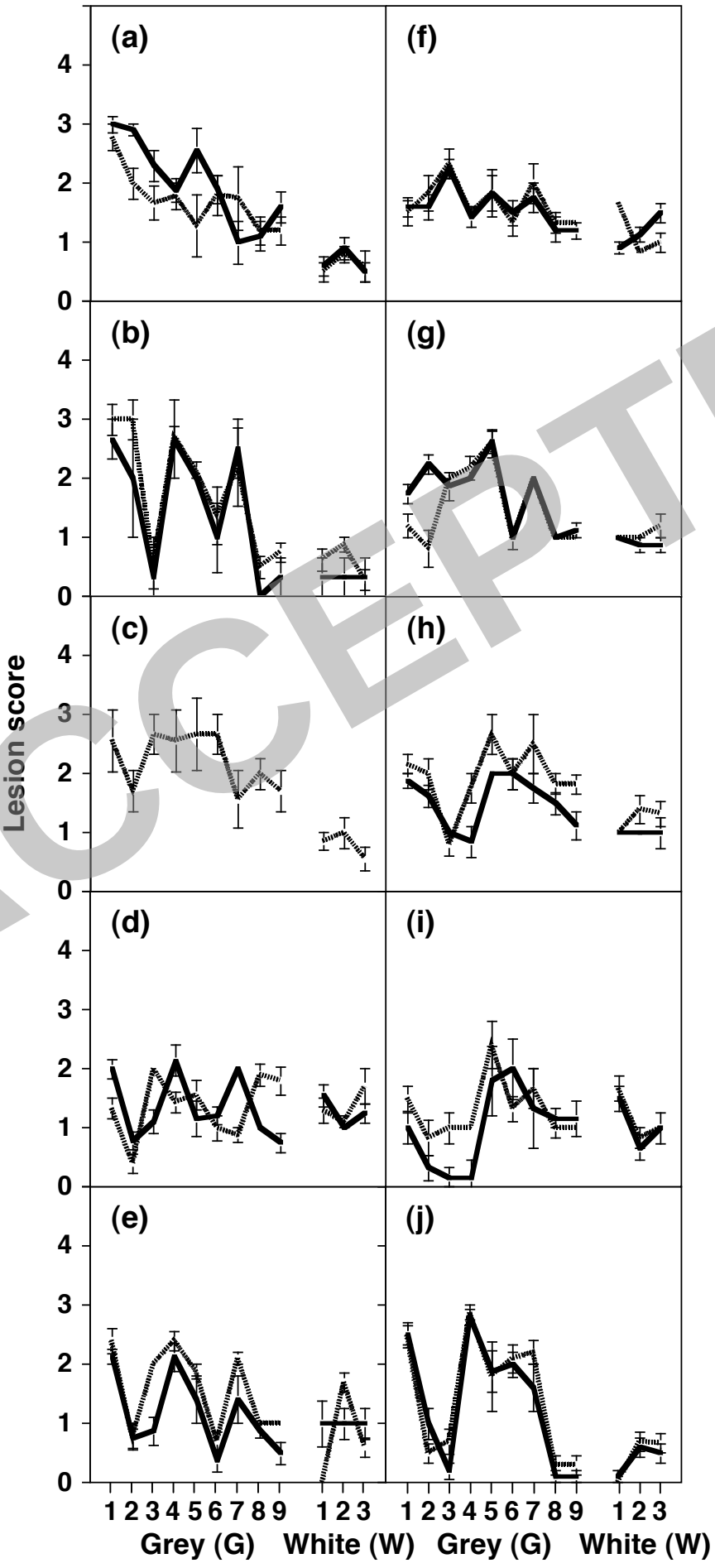

Table 2. Disease-associated PrP distribution in the brains of mice with terminal prion disease

Coronal Section	C57BL/6				VM				*tg59*				*tg338*			
	ARQ		VRQ		ARQ		VRQ		ARQ		VRQ		ARQ		VRQ	
	Part	Agg	Part	Agg	Part	Agg	Part	Agg	Part	Agg	Part	Agg	Part	Agg	Part	Agg
Frontal	+	+	+	-	+	+	+	-	+	+	+	-	+/-	-/+	-	-/+
Thalamic	+	+	+	-	+	+	+	-/+	+	+	+	-/+	+	-/+	+	+/-
Midbrain	+	+	+	-	+	+	+	-	+	+	+	-	+	-/+	+	-
Medulla	+	-/+	+	-	+	-/+	+	-	+	-/+	+	-	+	-/+	+	-

Figure 3. Immunohistochemistry of prion-infected mouse brains

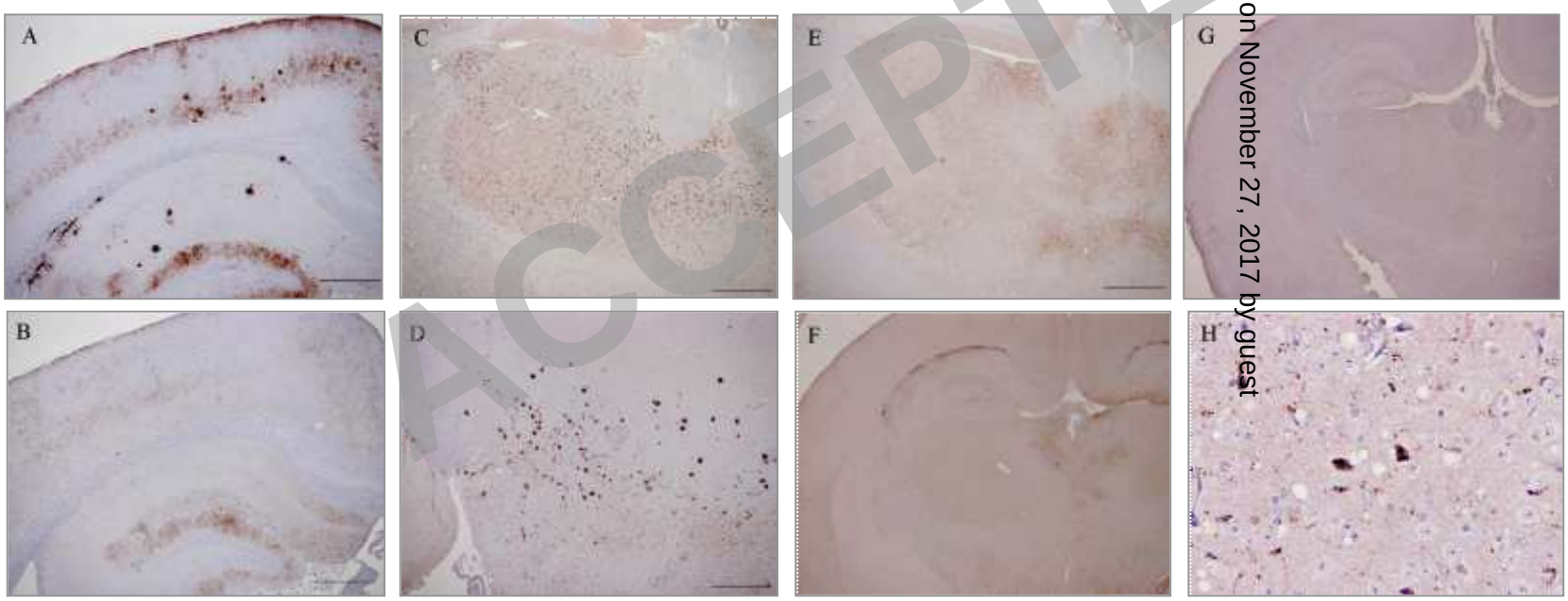

Figure 4. Relative levels of total PrPSc in prion-infected mouse brains measured by CDI

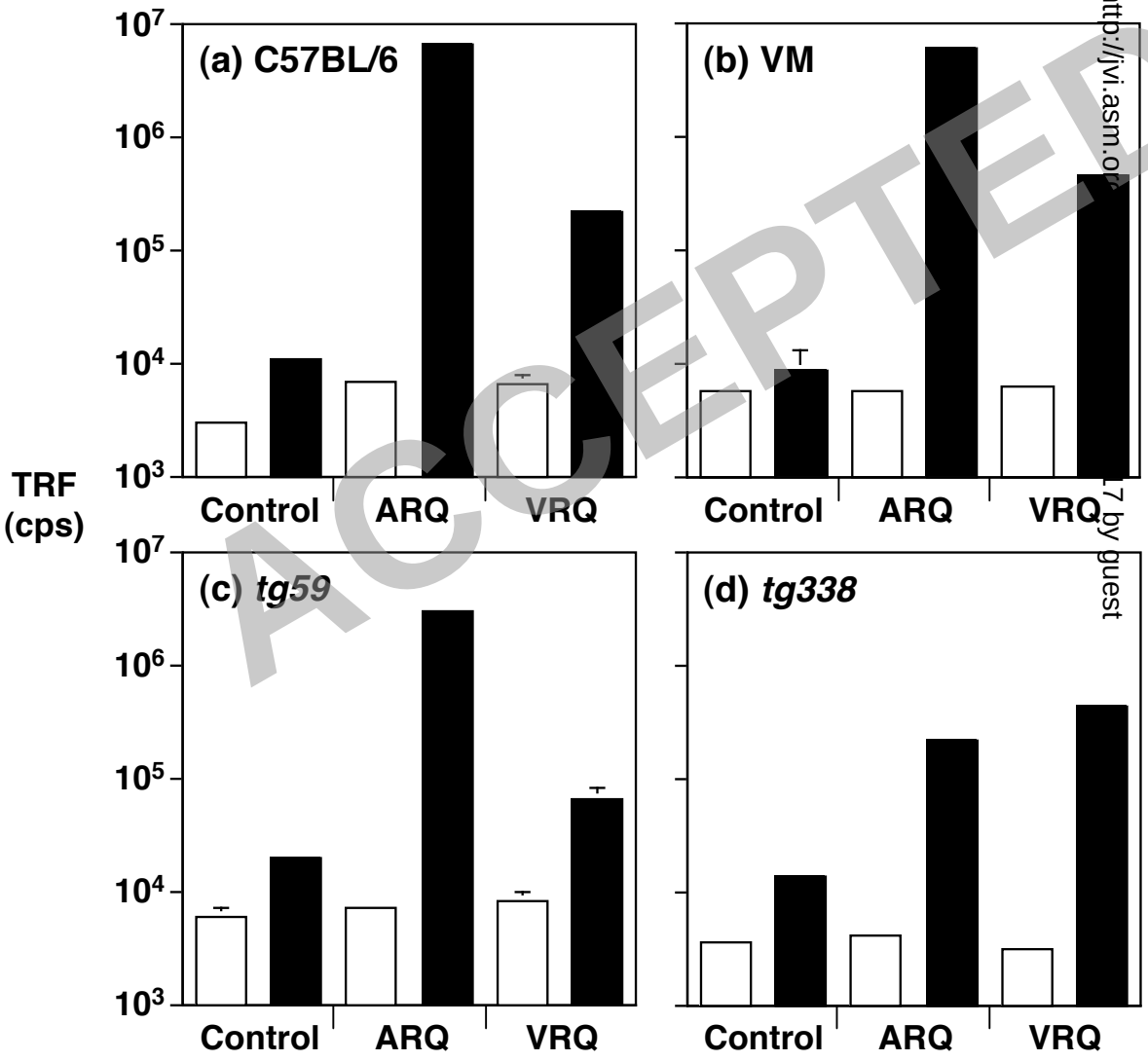

Figure 5. Western blot detection of PrP

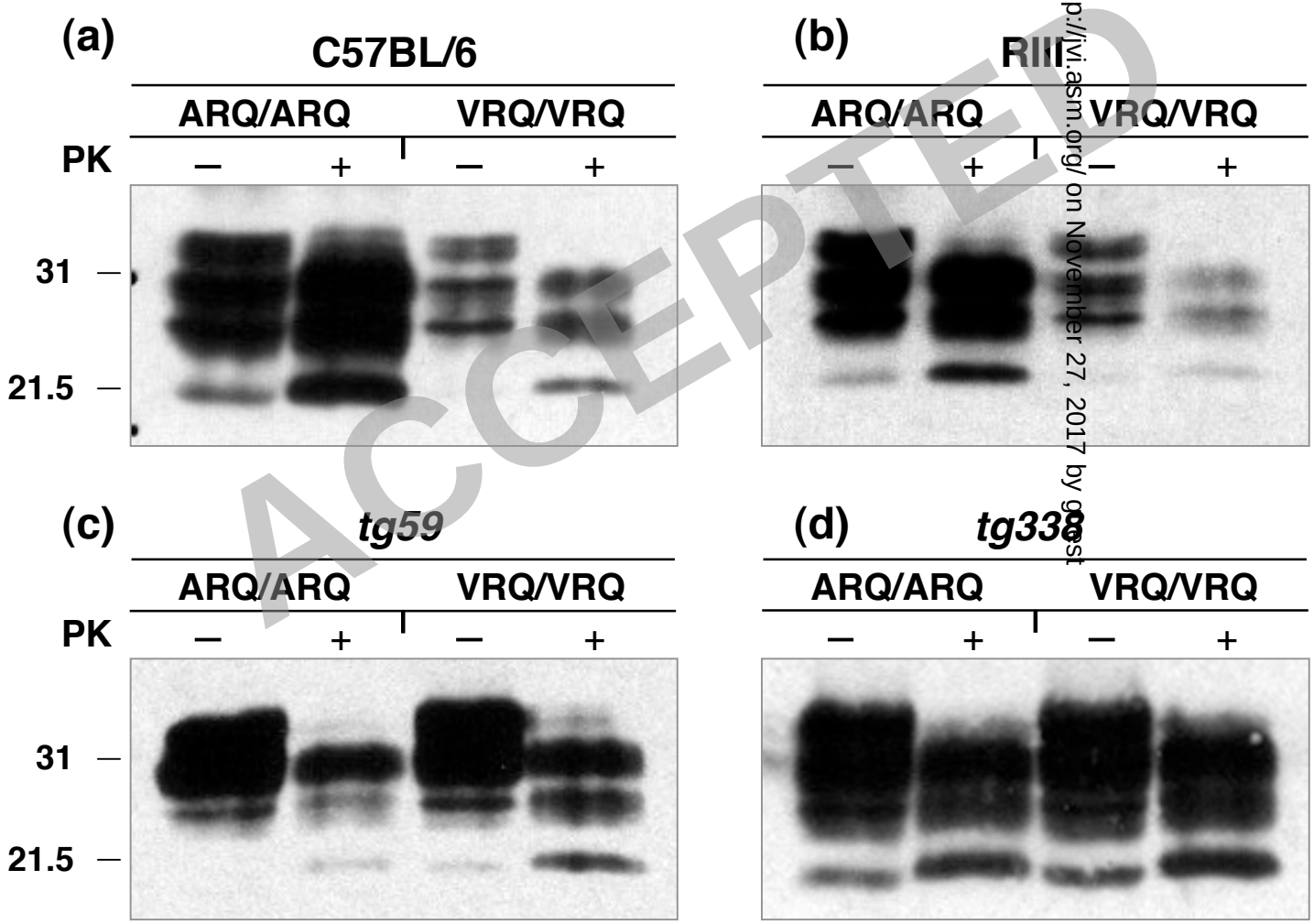

Figure 6. Conformational stability of ARQ- and VRQ-induced PrPSc